Pseudomorphic-to-close-packed transition. II. Application to Ni on Mo(110)

Jan H. van der Merwe, E. Bauer,* D. L. Tönsing, and P. M. Stoop
Department of Physics, University of South Africa, P.O. Box 392, Pretoria 0001, South Africa
(Received 2 August 1993)

The aim of this investigation is (a) to confirm by numerical quantification of analytical expressions in paper I, involving embedded-atom methods (EAM's), that a pseudomorphic, rather than a close-packed, Ni monolayer (ML) on Mo{110}, is stable, and (b) to establish the physics of the pseudomorphic-to-close-packed transition. Of the two close-packed configurations identified by a rigid-model approach, the one with incomplete misfit dislocations is shown, using transformed-stiffness constants (intralayer interaction) and EAM-calculated Fourier coefficients (interlayer interaction), to be the stable one with an average energy per Ni atom of 0.297 eV after final relaxation. An EAM calculation, presumably accounting for anharmonicity at 26% of pseudomorphic strain and for substrate proximity, yields the lower value 0.258 eV for the average energy per Ni atom in the pseudomorphic monolayer, and thus confirms the relative stability of the pseudomorphic monolayer. The pseudomorphic-to-close-packed transition—apparently from a lower energy pseudomorphic to a higher energy close-packed configuration—has been explained on kinetic grounds: the rapid formation of the close-packed configuration by penetration of excess atoms under nonequilibrium conditions of growth. Under equilibrium conditions, individual excess atoms reach the ML periphery by surface migration to effect continued pseudomorphic growth.

I. INTRODUCTION

In paper I (Ref. 1) we have described the phenomenon of interest; a Ni monolayer (ML) grows[2] at equilibrium pseudomorphically on a {110} Mo substrate—giving a (1×1) low-energy-electron-diffraction (LEED) pattern—until completion of one pseudomorphic (ps) ML. When atoms in excess of one ps ML are deposited a transition occurs to an almost close-packed (cp) ML which yields a (8×2) LEED pattern with misfit dislocations (MD's) at the Ni-Mo interface. In nonequilibrium growth, the ps-to-cp transition occurs already in ML islands even before completion of the ps ML.

The main objectives of this paper are, first, to show that the ps ML is more stable than the cp one and, second, to determine the physics governing the ps-to-cp transition. The primary effort here is to generate the numbers in support of our views.

II. NUMERICAL CALCULATIONS AND DISCUSSIONS

Growth mode

The first aspect of interest is the observed two-dimensional (2D) growth. The values[3] $\gamma_{Ni}=2.36\ \mathrm{J\,m^{-2}}$ and $\gamma_{Mo}=2.88\ \mathrm{J\,m^{-2}}$ of surface free energies are consistent with the 2D growth-mode criterion in Eq. (1) of Ref. 1, i.e., strong Ni-Mo, as compared to Ni-Ni, bonding. The latter figures strongly in the proposed physics governing the ps-to-cp transition to be dealt with below.

Geometry

The calculations are carried out for the geometry of Fig. 1 of Ref. 1. The empirical values of the nearest-neighbor distances, a of Mo and b of Ni, yield the values for the bulk misfits f_i. The MD densities $\bar{f}_i$ and misfit strains (MS's) $\bar{e}_i$ (see Eqs. (2)–(7) of Ref. 1) are obtained from the observed (1×1) and (8×2) LEED patterns. The results are displayed in Table I.

The following aspects of the data in Table I are notable: (i) the smallness of $|f_x|$, which suggests that the ML is subcritical,[4,5] i.e., $|f_x|<|f_x^c|$ in the x direction, accounts for the occurrence of the observed registry ($\bar{f}_x=0$) in both the ps and cp ML's; (ii) the large magnitude of the misfit strain ($\bar{e}_y\approx 26\%$) in the ps configuration, which (a) suggests that an anharmonic approach—embedded-atom method (EAM), in this case—might be needed to calculate the ps MS energy ϵ_{ps} and (b) facilitates the ps-to-cp transition in the

TABLE I. Bulk nearest-neighbor distances a (Mo) and b (Ni), volume per atom Ω (Ni), misfits f_i, misfit dislocation densities $\bar{f}_i$, and misfit strains $\bar{e}_i$ [$i=x,y$. See Eqs. (3)–(7) of Ref. 1], calculated from bulk lattice parameters.

	a (Å)	b (Å)	Ω (Å^3)	$r=b/a$	f_x	f_y	$\bar{f}_x$	$\bar{f}_y$	$\bar{e}_x$	$\bar{e}_y$
Bulk	2.726	2.489	10.9	0.9131	−0.0315	−0.209				
ps ML							0	0	0.0325	0.2646
cp ML							0	−0.2000	0.0325	0.0116

penetration—previously named climb[6]—of excess atoms into the ps ML; (iii) the large magnitude $|\bar{f}_y|$ of the MD density $\bar{f}_y$ in the cp ML, which could cause a degeneration of MD's into a misfit vernier (*MV*);[7] and (iv) the small MS $(\bar{e}_x,\bar{e}_y)$ in the cp ML—small enough to allow the use of the harmonic approximation in calculating the energetics of the cp ML.

Optimum Fourier coefficients

Proper quantitative considerations of the various issues require that the Fourier coefficients of the periodic ML atom-substrate interaction potential be known. Optimum coefficients[8] of the truncated series [Eq. (9) of Ref. 1] for the Ni-Mo interaction are calculated using the embedded-atom method potentials developed by Johnson.[9] The results are listed in Table II.

At this point, the following features of the quantities in Table II should be noted. (a) The bonding parameter A_0 is not only different for isolated and ML atoms but even more so for different material combinations, hence the name "bonding" parameter. (b) The values of the normalized coefficients A_i are dominated by the symmetry of the {110} bcc substrate. (c) In Eq. (9) of Ref. 1, only coefficients that operate in generating the Nishiyama-Wassermann orientation of fcc {111} on bcc {110} are included;[8] other terms with coefficients comparable to A_4 are ignored. This may be of significance if greater energy accuracy is needed. (d) A_3 is positive, whereas A_1 and A_4 are negative. This fact has significant consequences for the equilibrium configurations of the cp ML, as will be shown below.

Rigid-model energetics

Recall that the "rigid model" focuses[7] here on the energy of interaction of an extensive Ni{111} ML with a {110} Mo substrate, where the unit cell dimensions of the ML may be homogeneously varied, in which case the mismatch accommodation is by a MV. The energetics as analyzed in Sec. III A of Ref. 1—adopting the observed[2] registry constraint $\bar{f}_x=0$, i.e., $\bar{b}_x=a_x$ and the data in Table II—are displayed in Fig. 2 of Ref. 1. Shown in the figure are the average MV energies per ML atom: (a) $A_0=0.375$ eV when there is no registry at all, (b) $A_0[1-|A_1|(2-c_1+c_2)]=0.0236$ eV with full registry (ps: $\bar{f}_x=\bar{f}_y=0$), (c) $A_0(1+|A_1|c_1)=0.4335$ eV with registry $\bar{f}_x=0$ and ML atom y rows aligned along consecutive rows of adsorption sites [$x=0$ in Eq. (9) of Ref. 1], (d) $A_0(1-|A_1|c_1)=0.3165$ eV when the ML atom y rows of (c) are translated by $a_x/4$ in the x direction [see Eqs. (21) and (22) of Ref. 1], and (e) $A_0[1-|A_1|(c_1+c_2)]=0.2982$ eV when, for configuration (d), there is also row matching $\bar{f}_y=0$, i.e., $(\bar{b}_y=a_y)$ in the y direction. The translation $a_x/4$ in (d) decreases the average ML energy because A_3 is positive. The rigid-model analysis has thus identified two configurations for further analysis with the view to energy minimization, one with average energy per atom between 0.0236 and 0.4335 eV corresponding to the potential V_C of Eq. (22) of Ref. 1 and the other with average energy per atom between 0.2982 and 0.3165 eV corresponding to V_I in Eq. (21) of Ref. 1.

Energetics of misfit dislocations and misfit strain

In Sec. III A of Ref. 1, we concluded—accepting the observed[2] registry $\bar{f}_x=0$—that there are two candidates for minimum energy: a configuration with complete misfit dislocations (CMD's) and average energy per atom ϵ_C and one with incomplete misfit dislocations (IMD's) and average energy ϵ_I. From the foregoing section it now follows that approximately $0.0236<\epsilon_C<0.4335$ eV and $0.2982<\epsilon_I<0.3165$ eV. The precise values depend on the average energies ϵ_D of the MD's and $\epsilon_{\bar{e}}$ of residual MS. Because of the small corrugation height V_I^0 of IMD's $[V_I^0/V_C^0\approx c_2/2\approx 0.05$; Eqs. (21) and (22) of Ref. 1], it may be anticipated that the IMD's are closely represented by a MV (Ref. 7) with ϵ_I close to 0.3165 eV per atom, which is the average for the MV.

Because of the large amplitude V_C^0 of CMD's one may expect ϵ_D and $\epsilon_{\bar{e}}$ to be significant. The value of ϵ_C is obtained by adding ϵ_D and $\epsilon_{\bar{e}}$ to the lower limit 0.0236 eV. Whether ϵ_C is above or below ϵ_I can only be established by calculations of which the analytical part is given in Secs. III B–III E of Ref. 1. For the quantification of the analytical predictions we need values of both the Fourier coefficients in Eq. (9) of Ref. 1 and the elastic constants in Eq. (10b) of Ref. 1, respectively, listed in Tables II and III.

We first consider the stabilities of the ps and cp Ni ML's, constrained into $\bar{f}_x=0$ registry on Mo{110}. Of interest are (a) the critical misfits[4,5] f_y^c [Eqs. (39) and (50) of Ref. 1] below which a ps ML is stable against MS relief by introduction of MD's (CMD's and IMD's), (b) the nonequilibrium average energies $\epsilon_{\rm ne}^C$ and $\epsilon_{\rm ne}^I$ [Eqs. (35), (32), (47) and (51) of Ref. 1], respectively, for CMD's and IMD's at the MD density $\bar{f}_y=-0.2$, corresponding to the (8×2) LEED pattern,[2] (c) the averages $\epsilon_{\rm MV}^C$ and $\epsilon_{\rm MV}^I$—corresponding to the cases in (b)—for misfit accommodation by MV's, i.e., the MV energies $A_0(1\pm A_1|c_1)$ in Fig. 2 of Ref. 1, plus the strain $(\bar{e}_x,\bar{e}_y$; cp ML Table I) energies [Eq. (13a) of Ref. 1], (d) the energies $\epsilon_{\rm ps}^C$ and $\epsilon_{\rm ps}^I$ of a ps Ni ML (≡corresponding minima

TABLE II. Optimum Fourier coefficients of Eqs. (9) of Ref. 1: (a) an isolated Ni atom and (b) a Ni atom in a rigid ML.

		A_1	$A_3=-A_1c_1$	$A_4=A_1c_2$	$c_1=-A_3/A_1$	$c_2=A_4/A_1$	A_0 (eV)
Ni on	(a)	−0.535	0.163	−0.039	0.305	0.073	0.436
Mo{110}	(b)	−0.522	0.156	−0.049	0.299	0.094	0.375

TABLE III. Empirical bulk c_{ij} and derived elastic constants $\bar{c}_{ij}$ ($\times 10^{11}$ dyn cm^{-2}), ratios P and R, and product $\Omega\bar{c}_{11}$ in eV per atom [see Eqs. (13) of Ref. 1] for a Ni{111} monolayer. P and R are dimensionless.

c_{11}	c_{12}	c_{44}	$\bar{c}_{11}$	$\bar{c}_{12}$	$\bar{c}_{66}$	P	R	$\Omega\bar{c}_{11}$
23.2	14.8	11.2	30.20	12.47	8.87	0.418	0.294	20.85

$A_0[1-|A_1|(2-c_1+c_2)]$ and $A_1[1-|A_1|(c_1+c_2)]$ plus the strain ($\bar{e}_x,\bar{e}_y$; ps ML in Table I) energies Eq. (13a) of Ref. 1). In all cases the transformed bulk elastic constants of Table III have been used in calculating the desired quantities.

The following features of the results listed in Table IV are relevant. (a) The magnitudes $|f_y^c|$ of critical misfits (16 and 7%) are not only well below the existing bulk value of 21% applicable to Ni on Mo but, in addition, $|f_y^{cI}|$ is significantly less than $|f_y^{cC}|$ as may be anticipated on the grounds of the difference in corrugation heights V_I^0 and V_C^0 [Eqs. (21) and (22) of Ref. 1] of the corresponding potentials. (b) for IMD's (relatively small V_I^0) the energies per atom $\epsilon^I=0.328$ eV in the cp ML differ by only about 0.1% for the observed (8×2) LEED pattern when calculated for misfit accommodation by MD's and a MV. For CMD's with (relatively large V_C^0) the energy $\epsilon^C\equiv\epsilon^C_{\rm ne}=0.413$ eV is almost 8% less than the value for the MV. (c) That $\epsilon^I_{\rm ps}>\epsilon^C_{\rm ps}$, even though $|f_y^{cI}|<|f_y^{cC}|$, is due to the relatively big difference in the bottom levels $A_0[1-|A_1|(c_1+c_2)]$ and $A_0[1-|A_1|(2-c_1+c_2)]$ (see Fig. 2 of Ref. 1), the configuration generating IMD's being constrained by the ridgid translation $\Delta x=a_x/4$.

The foregoing allows some important conclusions. (i) The fact that the calculated values of $\epsilon_{\rm cp}$ are fairly reliable—the Fourier coefficients are fairly reliable and the strains ($\bar{e}_x,\bar{e}_y$; cp ML in Table I) are adequately within the harmonic regime—justifies the conclusion that the difference between 0.413 and 0.328 eV may be taken as sufficient proof that a cp ML with IMD's is more stable than one with CMD's. For relaxation beyond the zero-order approximation we may accordingly restrict ourselves below to IMD's. (ii) The fact that $\epsilon^I_{\rm ps}$ is significantly larger than $\epsilon^C_{\rm ps}$ identifies the configuration with adatoms in adsorption sites as the appropriate ps configuration, as expected. (iii) That $\epsilon^C_{\rm ps}$ is still significantly larger than $\epsilon^I_{\rm cp}$ is inconsistent with the observations.[2] We suggest that the harmonic approximation, used in the calculation, grossly overestimates $\epsilon_{\rm ps}$ and that an anharmonic approach be used to calculate $\epsilon_{\rm ps}$. We believe that an EAM calculation, though crude, is an adequate anharmonic approximation.

Energetics of relaxed IMD's

We first pursue the energetics of the cp configuration as IMD's relax (Sec. III E of Ref. 1). By using the definitions in Eqs. (2b) of Ref. 1, the parameter values from Tables I–III, and the value $J=10$ for the (8×2) LEED pattern, we obtain for the quantities in Eqs. (57) of Ref. 1 the values $\alpha=0.4899$, $\bar{\alpha}=0.3404$, and $\beta=0.4439$ and, hence, for Eqs. (58) of Ref. 1 approximately

$$\begin{aligned} &0.5126a_1+0.0986b_2=0.06274\\ &-1.6970a_2+0.0986b_1=0\\ &-0.0948a_1+0.0580a_2-0.4057b_1=0\\ &0.0580a_1-0.3790a_2-1.5791b_2=0.00347\ . \end{aligned} \tag{1}$$

When the solutions ($a_1=-0.1238$, $a_2=0.00169$, $b_1=0.02914$ $b_2=-0.00714$) of Eq. (1), together with values from Tables I–III, are substituted into Eqs. (60)–(62) of Ref. 1, we obtain approximately $V_0^{\rm av}=0.3165$ eV, $\bar{\epsilon}_0^{\rm av}=0.0157$ eV, $\Delta V=-0.0691$ eV, $\Delta\bar{\epsilon}=0.0331$ eV, and, hence, for the energy of related IMD's the value $\bar{\epsilon}^I_{\rm rel}=0.2962$ eV per Ni atom. This value, which we take as $\epsilon_{\rm cp}$, is shown in Table IV. The energy of relaxation 0.033 eV is seen to be about 10% of the MV energy 0.332 eV per atom. The nature of the atomic configuration with relaxed IMD's, as based on the calculated values of a_i and b_i, is modeled in Fig. 5 of Ref. 1. It is significant that these results agree well with the more limited results from two quite different theoretical treatments of a similar film-substrate system, Pd/Nb{110}; an electronic structure calculation[10,11] and a molecular-dynamics/Monte Carlo study.[11]

Anharmonic strain energy

We now turn to calculating the anharmonic strain ($\bar{e}_y\approx 26\%$) energy, using the EAM's developed by Johnson.[9] An important feature of this calculation, apart from anharmonicity, is that the ML is strained (extended or contracted) with respect to the rigid substrate surface when MS is introduced, in contrast to the atomic layers

TABLE IV. The table displays (a) the percentage of critical misfits f_y^c and (b) the average energies per Ni atom ϵ in eV, where the superscripts C denote CMD and I denote IMD, subscripts ne denote nonequilibrium ML with $\bar{f}_y=-0.20$ [the (8×2) LEED pattern], and MV denotes misfit vernier with $\bar{f}_y=-0.2$—all ϵ's representing possible values of $\epsilon_{\rm cp}$—and subscript ps denotes pseudomorphic defining $\epsilon_{\rm ps}$. In all cases, $\bar{f}_x$ is taken as zero and bulk elastic constants are used. The energy $\epsilon^I_{\rm relax}$, when IMD are relaxed, is shown $\epsilon_{\rm cp}$ and the EAM-calculated ps energy as $\epsilon_{\rm ps}$.

f_y^{cC}	f_y^{cI}	$\epsilon^C_{\rm ne}$	$\epsilon^C_{\rm MV}$	$\epsilon^I_{\rm ne}$	$\epsilon^I_{\rm MV}$	$\epsilon^C_{\rm ps}$	$\epsilon^I_{\rm ps}$	$\epsilon_{\rm cp}$	$\epsilon_{\rm ps}$
−16	−7	0.413	0.446	0.328	0.331	0.840	1.113	0.297	0.258

in a homogeneously strained bulk crystal where all layers are strained by the same amount. This aspect of the calculation is handled by noting that the electron density [see Eq. (14) of Ref. 1] emanating from the substrate (taken rigid) is a periodic function of position in the plane of the ML and that the ML atoms accordingly experience from the substrate a periodic electron density when the ML is misfit strained. It has been shown[12] that the interaction of epilayer atoms with the substrate when calculating the harmonic and anharmonic properties of an extensive supported ML can be adequately accounted for in terms of the averages of electron density ρ and pair potential ϕ in the plane of the ML. The total energy of the epilayer-substrate system during epilayer deformation involves, likewise, the interaction of substrate-layer atoms with the deforming ML, as well as intralayer interactions. It follows from these considerations that an unsupported ML, a supported ML, and a ML forming part of the bulk will experience different energetics when strained similarly. Their strain energies, equilibrium lattice parameters, and elastic constants would be different, the main reason being the role of the electron density in the embedding energy. For the present, it suffices to say that the values of the relevant quantities are smallest for the supported ML. The dependence of strain energy ϵ^C on strain $\bar{e}_y$, where $\bar{e}_y$ is measured with respect to bulk lattice parameters and $\bar{e}_x=0.0325$ ($\bar{f}_x=0$), is shown in Fig. 1. Special features of the curve are that (a) the minimum of ϵ^C occurs at $\bar{e}_y\approx 0$—if completely free to relax in the ML plane, it is stable at $\bar{e}_x=\bar{e}_y\approx 0.012$, i.e., an expansion with respect to the bulk; (b) the dependence of ϵ^C on $\bar{e}_y$ is almost linear over a wide range—the reason is not obvious; and (c) $\epsilon^C_{ps}\simeq 0.235$ eV. For comparison with ϵ_{cp} we still have to add the ML atom-substrate energy 0.0236 eV at the adsorption sites; hence, $\epsilon_{ps}=0.258$ eV, which is well below the value of $\epsilon_{cp}=0.297$ eV obtained above. The calculated values of ϵ_{ps} and ϵ_{cp} are accordingly consistent with the observation[2] that the ps ML is stable. It is notable that ϵ_{ps} is drastically below the harmonic value ϵ^C_{ps} in Table IV. This is due to anharmonicity and substrate proximity.

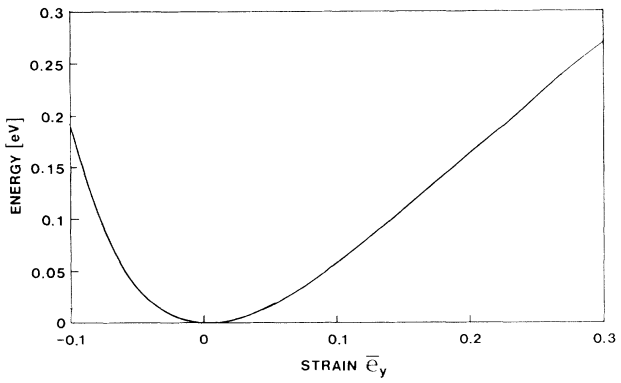

FIG. 1. Plot of the strain energy (eV) of a Ni ML on a Mo{110} substrate vs ML strain $\bar{e}_y$ (measured relative to bulk Ni lattice dimensions) in the y direction when constrained to registry ($\bar{f}_x=0$, $\bar{e}_x\approx 0.0325$) in the x direction. The energy minimum is seen to occur close to $\bar{e}_y=0$. When no constraints are imposed the ML configuration is stable at $\bar{e}_x=\bar{e}_y\approx 0.012$. At the ps strain $\bar{e}_y\approx 0.265$ the average strain energy per atom with $\bar{e}_x=0.0325$ is approximately 0.235 eV.

Physics of the ps-to-cp transition

We now address the following question: if the ps ML is more stable (is of lower energy) than the cp one, how can we explain that a cp configuration forms, rather the continued growth of the ps ML, when excess atoms are deposited on top of the ps ML? There is a combination of keys to the understanding of this phenomenon, the main keys being strong Ni-Mo bonding, large ($\approx 26\%$) ps strain, and kinetics, which we now discuss in some detail.

It has been shown previously[6] that adatoms on top of a ps ML may penetrate the ML to introduce strain-relieving MD's, that stability of a ML requires the presence of MD's when the misfit exceeds the critical misfit, that the critical nucleation length of a MD is about one atom, and that the nucleation energy at critical misfit is approximately

$$W_A=\mu\Omega/4 \tag{2}$$

in an isotropic ML with quadratic lattice symmetry, when the intralayer and interlayer interactions are similar, μ and Ω being, respectively, the shear modulus and volume per atom. For Ni on Ni, $W_A\approx 1$ eV. It follows from Tables I and IV that the magnitudes of the critical misfits for Ni on Mo, particularly $|f_y^{cI}|$, are well below the bulk value $|f_y|\approx 21\%$. One would therefore expect the penetration mechanism to be active for the Ni ML on Mo, there being strong Ni-Mo bonding and excessive ps strain. In fact, a calculation[6] using the EAM's developed by Johnson[9] shows that the penetration mechanism is almost spontaneous in this case.

There is an important retarding factor to the transition mechanism proposed above: the stable cp configuration is one with IMD's, which requires a rigid translation $\Delta x=a_x/4$ relative to the ps configuration. This process should involve an energy of activation. The captured adatom may accordingly escape in time to the surface and be recaptured elsewhere or eventually migrate to the periphery of the ML where it contributes to the growth of the ps configuration. It is proposed that the proximity of enough excess atoms is necessary for the generation of stable finite length IMD's and the formation of pseudostable finite-sized cp domains. Since domains form independently, neighboring domains may correspond to opposite rigid displacements and form domain boundaries constituting positive line energies.

A different but somewhat related mechanism for the formation of such domain (grain) boundaries was proposed by Kołaczkiewicz and Bauer[13] for the observed transition from a ps to a coincident (near cp) structure of absorbed Ni on W(110). Their proposal stems from the observation that in annealed layers the transition occurs at higher coverages, which suggests that larger ps ML islands are more stable than smaller ones. They pointed out that if ps ML islands were to form by adsorption ei-

ther at threefold "surface sites" or at bridge sites, then coalescing islands, which have formed on different sets of such sites, would be separated by domain (grain) boundaries. The grain-boundary energies would provide the driving forces for the transition—they would be more effective for small than for large islands. The validation of this proposal still awaits confirmation of the proposed adsorption.

On the basis of these considerations we propose the following understanding of the observed phenomena. Under quasiequilibrium conditions an excess adatom on top of a ps ML will eventually reach the periphery of the ML where it effects growth of the stable ps configuration. Under nonequilibrium conditions—high deposition rate and/or low substrate temperature—a sufficient density of excess atoms builds up so that pseudostable cp domains, containing finite-length IMD's, may form by the penetration mechanism. Two additional features, in support of the penetration mechanism, need be noted: first, the penetration displacement of about one atomic spacing is negligible as compared to the hundreds and more for reaching the periphery, and second, the decrease in free energy due to the configuration entropy of the more-or-less random distribution of finite length IMD's. These considerations also explain the occurrence of the ps-to-cp transition in finite sized ML islands under nonequilibrium conditions.[2]

It is suggested that the return to the stable ps configuration is effected by the escape of IMD's at the periphery of the cp ML. This again requires prolonged annealing as the process is retarded by activation barriers at the periphery and the cancellation of the rigid displacements.

We may conclude by pointing out that what we are actually comparing are three different configurations—a ps ML with excess atoms on top, a cp ML with the extra atoms at IMD's, and an enlarged ps ML containing the excess atoms—of the same system comprising a given number of Ni atoms deposited on a Mo{110} substrate. The corresponding energies of the three configurations decrease in the order listed above. The succession of transitions characterized by this order constitutes the favorable kinetic path under nonequilibrium conditions.

III. SUMMARY AND CONCLUSIONS

The main objectives of this investigation are (a) to confirm analytically and computationally the empirical conclusion that the ps Ni ML on Mo{110} is stable (if of less energy than the cp one) and (b) to determine the physical basis of the ps-to-cp transition. These phenomena, which should also be obtained for the growth of Cu and Co on Mo and W(110), have been dealt with under the following categories.

(A) Growth mode. The observed 2D growth, even for a cp ML, was shown to be consistent with equilibrium criteria[14] and is evidence for strong Ni-Mo bonding.

(B) Stability. (1) Strong Ni-Mo bonding and small misfit ($f_x \approx -3\%$) is consistent with one-dimensional misfit accommodation by MS ($\bar{e}_x \approx 3\%$) in the x direction for both the ps and cp configurations. (2) Optimum Fourier coefficients (OFC's) for the periodic Ni-atom–Mo-substrate interaction are computed using EAM's. (3) OFC's are used in conjunction with the rigid model to identify two candidates for the minimum-energy cp configuration. (4) The two candidates of item (3) have been described in terms of CMD's, involving a displacement vector of diagonal length a_y, and IMD of displacement vector $a_y/2$, and a rigid displacement $\Delta x = \pm a_x/4$. These are quantified using the OFC's of item (2) and a harmonic approach. A zero-order approximation in which the atomic rows parallel to y are constrained to be straight showed convincingly that the cp configuration with IMD's is the stable one (energies per atom of 0.328 and 0.413 eV).

(5) By a first-order approximation in which the atoms in the y rows are allowed transverse displacements, the average energy per atom with IMD's is reduced to 0.297 eV. This is taken as the energy per atom ($\epsilon_{cp} \approx 0.297$ eV) of the cp configuration.

(6) EAM calculations, accounting for anharmonicity and substrate proximity, yields the value $\epsilon_{ps} \approx 0.258$ eV for the energy of the highly strained ($\bar{e}_y \approx 26\%$) ps ML.

(7) The excess of ϵ_{cp} over ϵ_{ps} is taken as adequate proof of the stability of the ps ML.

(C) Physics of the ps-to-cp transition. (1) It is proposed that the ps-to-cp transition is effected by the penetration of excess atoms into the ps ML to form a cp configuration with IMD's. (2) Excess atoms participate in two competing processes: penetration to generate the cp configuration and surface migration towards the ML periphery to effect continued ps growth. (3) The penetration mechanism is facilitated by a sufficient density of excess Ni atoms (nonequilibrium conditions), strong Ni-Mo bonding, large ($\bar{e}_y \approx 26\%$) ps strain, and the configurational entropy of the random distribution of finite-length IMD's within cp domains, but retarded by activation barriers, particularly the barrier associated with the rigid translation ($\Delta x = \pm a_x/4$). (4) Under quasiequilibrium conditions (low deposition rate and/or adequate substrate temperature) individual excess Ni atoms may cover the relatively large distance to the ML periphery to ensure continued ps growth. (5) The degree of nonequilibrium, i.e., kinetics, determine whether continued ps growth is maintained or whether a ps-to-cp transition occurs. Kinetics determine whether there would be a direct transition between a ps ML with excess atoms on top to a larger ps ML or the transition occurs via a cp configuration.

(D) Reliability. The quantification of the relevant quantities, allowing the predictions, is accomplished with the aid of EAM's. It is admitted that the accuracy of this description is open to criticism. EAM's have been applied previously though with a fair degree of success in calculating surface properties, and a similar degree of success may be expected here. Also, since the same EAM's are used for all quantities, it is proposed that qualitatively they allow the correct conclusions, although the individual quantities may carry errors, believed to be not more than 10%. We also propose that the present considerations define analytical and computational procedures that can be useful in a more fundamental and accurate description of atomic interactions.

*Permanent address: Physikalisches Institut der Technischen Universität Clausthal, D-38698 Clausthal-Zellerfeld, Germany.

[1]J. H. van der Merwe and E. Bauer, preceding paper, Phys. Rev. B **49**, 2127 (1994).
[2]M. Tikhov and E. Bauer, Surf. Sci. **232**, 72 (1990).
[3]L. Z. Mezey and J. Giber, Jpn. J. Appl. Phys. **21**, 1569 (1982).
[4]F. C. Frank and J. H. van der Merwe, Proc. R. Soc. London Ser. A **198**, 205 (1949); **198**, 216 (1949).
[5]J. H. van der Merwe, J. Appl. Phys. **41**, 4725 (1970).
[6]D. L. Tönsing, P. M. Stoop, and J. H. van der Merwe, Surf. Sci. **277**, 193 (1992).
[7]J. H. van der Merwe, Philos. Mag. **45**, 145 (1982).
[8]P. M. Stoop, J. H. van der Merwe, and M. W. H. Braun, Philos. Mag. B **63**, 907 (1991).
[9]R. A. Johnson, Phys. Rev. B **39**, 12 554 (1989); **41**, 9717 (1990).
[10]V. Kumar and K. Bennemann, Phys. Rev. B **26**, 7004 (1982); **28**, 3138 (1983).
[11]B. C. Bolding and E. A. Carter, Phys. Rev. B **42**, 11 380 (1990); **44**, 3251 (1991).
[12]J. H. van der Merwe, D. L. Tönsing, and P. M. Stoop, Surf. Sci. (to be published).
[13]J. Kołaczkiewicz and E. Bauer, Surf. Sci. **144**, 495 (1984).
[14]E. Bauer, Z. Kristallogr. **110**, 372 (1958).